



Meromorphic functions and the topology of giant gravitons



Michael C. Abbott^{a,*}, Jeff Murugan^a, Andrea Prinsloo^b, Nitin Rughoonauth^{a,c,d}

^a Laboratory for Quantum Gravity & Strings, Department of Mathematics & Applied Mathematics, University of Cape Town, Rondebosch 7701, South Africa

^b Department of Mathematics, University of Surrey, Guildford, GU2 7XH, United Kingdom

^c Max-Planck-Institut für Physik, Föhringer Ring 6, 80805 Munich, Germany

^d Arnold-Sommerfeld-Center für Theoretische Physik, LMU München, Theresienstraße 37, 80333 Munich, Germany

ARTICLE INFO

Article history:

Received 19 December 2013

Accepted 21 January 2014

Available online 31 January 2014

Editor: M. Cvetič

ABSTRACT

Using Mikhailov's map from holomorphic functions to supersymmetric D3-brane solutions, we show how to construct giant gravitons in $AdS_5 \times S^5$ with toroidal topologies. In the $\frac{1}{4}$ -BPS sector we show that these are always of the form $\#^K(S^2 \times S^1)$, and in the limit in which this becomes a set of $m+n$ perpendicular spherical giants re-connected near to their intersections, we find K in terms of m, n . In the $\frac{1}{8}$ -BPS sector we find a similar class of solutions.

© 2014 The Authors. Published by Elsevier B.V. Open access under CC BY license. Funded by SCOAP³.

1. Introduction

The best understood sector of AdS/CFT [1] concerns closed fundamental strings, which in the gauge theory are single-trace operators of length much less than N [2]. D-branes are heavier objects corresponding to operators of length order N , the most studied of which are spherical branes known as giant gravitons [3], dual to determinant operators and generalisations known as Schur polynomials [4–6].

The worldsheet of any closed string state is a cylinder $\mathbb{R} \times S^1$, but for D3-branes any $\mathbb{R} \times \mathcal{M}$ is in principle possible, with \mathcal{M} a closed 3-manifold. Such manifolds can have considerably more complicated topology than closed 1-manifolds, and it would be fascinating to understand the emergence of topology from the dual SYM operators. Motivated by this, the goal of this Letter is to explore what topologies occur in giants with a given amount of supersymmetry. We are particularly interested in solutions created by a localised modification of a set of intersecting spherical giant gravitons, as this seems the most tractable limit.

We begin by recalling the map given by Mikhailov [7,8]: Any analytic function $f: \mathbb{C}^3 \rightarrow \mathbb{C}$ defines a supersymmetric D3-brane solution in $\mathbb{R} \times S^5 \subset AdS_5 \times S^5$ as the surface

$$f(e^{-it}Z_1, e^{-it}Z_2, e^{-it}Z_3) = 0, \quad \sum_i |Z_i|^2 = 1 \quad (1)$$

where $Z_i = r_i e^{i\phi_i}$ are the 3 complex embedding co-ordinates for S^5 . The degree of supersymmetry is given by the number of arguments: $f(Z_1)$ gives a $\frac{1}{2}$ -BPS solution, $f(Z_1, Z_2)$ $\frac{1}{4}$ -BPS, and $f(Z_1, Z_2, Z_3)$ gives a $\frac{1}{8}$ -BPS solution.

The usual sphere giant graviton is given in this language by

$$f(Z_1) = Z_1 - \alpha. \quad (2)$$

This constrains Z_1 completely, so the worldvolume (at a given time) is the S^3 parameterised by Z_2 and Z_3 subject to $|Z_2|^2 + |Z_3|^2 = 1 - \alpha^2$. The only time-evolution is that it rotates in the Z_1 plane; the maximal giant graviton has $\alpha = 0$ and is thus stationary, while in the opposite limit $\alpha \rightarrow 1$ the brane collapses down to a point particle on a lightlike trajectory. A function $f(Z_1)$ with several zeros will lead to a number of concentric spherical giants.

We refer to (2) as the case (1, 0, 0): one Z_1 giant. The next section studies the effect of adding to this terms depending on Z_2 , and then takes a limit in which these give n intersecting Z_2 giants: cases (1, n , 0). After that we consider arbitrarily many intersecting Z_1 and Z_2 giants, cases ($m, n, 0$) (Section 3), and finally the addition also of Z_3 giants (Section 4). We give a concise statement of our results in Section 5.

2. Quarter-BPS class (1, n , 0)

To begin constructing topologically nontrivial solutions using Mikhailov's method, in this section we add to the spherical giant's $f(Z_1)$ a meromorphic function of Z_2 . Consider first the function

$$f(Z_1, Z_2) = Z_1 - \alpha + \frac{\epsilon}{Z_2}. \quad (3)$$

* Corresponding author.

E-mail addresses: michael.abbott@uct.ac.za (M.C. Abbott), jeff@nassp.uct.ac.za (J. Murugan), a.prinsloo@surrey.ac.uk (A. Prinsloo), nitinr@gmail.com (N. Rughoonauth).

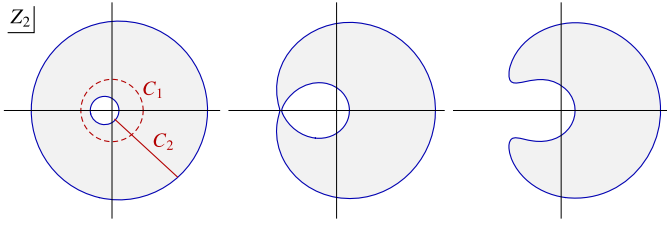


Fig. 1. Plots showing the area Σ of the Z_2 plane which is covered by the D3-brane specified by (3). Increasing the residue, we progress from a torus $\mathcal{M} = S^2 \times S^1$ via the critical case to a deformed S^3 . Parameters are $\alpha = \frac{1}{2}$ and $\epsilon = \frac{1}{10}, 0.1844, \frac{1}{5}$.

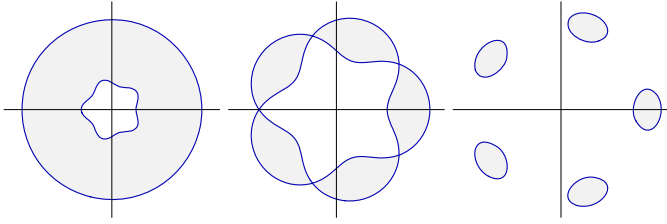


Fig. 2. Plots showing Σ with one quintuple pole, (5) with $N = 5$. Increasing ϵ we pass from the torus on the left to five spheres on the right; the middle picture is close to ϵ_{crit} . Parameters are $\alpha = \frac{1}{2}$ and $\epsilon = \frac{1}{1000}, 0.03833, \frac{1}{5}$.

We may assume $\alpha, \epsilon > 0$ and, since the motion of the brane is rigid, we need only discuss its topology at time $t = 0$.

Let us parameterise the D3-brane worldvolume by the ϕ_3 circle and some portion of the Z_2 plane. (Solving $f = 0$ fixes Z_1 in terms of Z_2 , and $\sum_i r_i^2 = 1$ fixes r_3 .) We can read off the topology of the brane from the topology of the area of the Z_2 plane thus covered: let Σ be the area where $r_3(Z_2)^2 \geq 0$. For example, the spherical giant graviton (2) clearly has for Σ the disk $|Z_2| \leq 1 - \alpha^2$.

The effect of turning on the pole is to make a hole in the base space Σ , thus increasing its genus (see Fig. 1). This may be understood by saying that in a neighbourhood of the pole, the term ϵ/Z_2 is so large that there are no solutions $|Z_1| \leq 1$. Notice immediately that this means that the pole itself is not on the worldvolume of the brane.

To analyse this more carefully, it is easy to show using (3) that Σ is given by

$$r_2^4 + r_2^2(\alpha^2 - 1) + \epsilon^2 \leq 2\epsilon\alpha r_2 \cos\phi_2. \quad (4)$$

Drawing graphs of the left- and right-hand sides in terms of r_2^2 , when $\epsilon = 0$ certainly there are two intersections. Increasing ϵ , there is a range $0 < \epsilon < \epsilon_{\text{crit}}$ in which there are two intersections $r_2 > 0$ for all ϕ_2 , followed by a range $\epsilon_{\text{crit}} < \epsilon < \epsilon_{\text{max}}$ in which there are two intersections at $\phi_2 = 0$ but not at $\phi_2 = \pi$. For larger ϵ there are no intersections. This progression is shown in Fig. 1.

For $\epsilon < \epsilon_{\text{crit}}$ the topology of the brane is $S^2 \times S^1$. The incontractible cycle C_1 (more or less the ϕ_2 circle) is the S^1 factor, while a radial line in Σ gives the S^2 factor – this is an interval fibred with the ϕ_3 circle, which shrinks to zero at either end. It is marked C_2 in the figure.

The simplest generalisation is to consider a higher-order pole:

$$f(Z_1, Z_2) = Z_1 - \alpha + \frac{\epsilon}{(Z_2)^N}. \quad (5)$$

This leads to the same topology as the single pole, for small ϵ , but the geometry has a symmetry $Z_2 \rightarrow e^{i2\pi/N} Z_2$. Because of this, in the regime $\epsilon_{\text{crit}} < \epsilon < \epsilon_{\text{max}}$ there will be N separate (deformed) 3-spheres. Fig. 2 shows the case of $N = 5$.

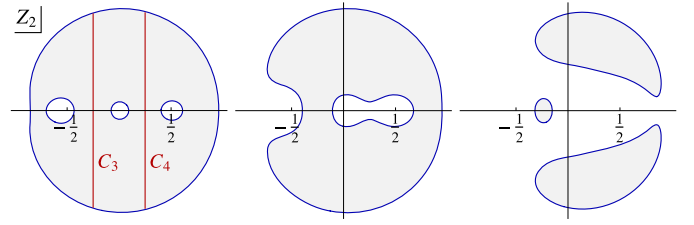


Fig. 3. Plots showing Σ for the case (1, 3, 0), using (6) with three poles at $\beta_1 = -\frac{1}{2}$, $\beta_2 = 0$ and $\beta_3 = \frac{1}{2}$. The residues are $\epsilon, \epsilon, -\epsilon$ respectively, with ϵ increasing from $\frac{1}{12}$ (left, giving $\mathcal{M} = \sharp^3(S^2 \times S^1)$) to $\frac{1}{3}$ (centre, giving $S^2 \times S^1$) to $\frac{1}{3}$ (right, $\sqcup_3 S^3$), and $\alpha = \frac{1}{2}$. Notice that the holes in Σ formed by residues of opposite signs attract, while those of the same sign repel. The lines C_3, C_4 in Σ each lift to a separating S^2 in \mathcal{M} .

We can also consider several poles:

$$f(Z_1, Z_2) = Z_1 - \alpha + \sum_{j=1}^n \frac{\epsilon_j}{Z_2 - \beta_j}. \quad (6)$$

For small enough ϵ_j the analysis very close to each pole will be similar to that for one pole: expanding in $r_{2\beta} = |Z_2 - \beta_j|$ will give us (4) plus terms of higher order in $r_{2\beta}$. Thus for any set of n poles (located at β_j such that $\alpha^2 + |\beta_j|^2 < 1$) there exist residues $\epsilon_j \neq 0$ such that Σ is a disk with n holes. Cutting Σ along lines such as C_3, C_4 in Fig. 3, so that each hole is isolated, we see that the resulting topology is a connected sum¹

$$\mathcal{M} = \sharp^n(S^2 \times S^1). \quad (7)$$

Note that all poles are outside Σ , so everywhere on the worldvolume the function f is analytic.

With multiple poles the progression as we increase ϵ_j can be quite complicated, and can produce several disconnected pieces. The case of poles at $Z_2 = 0, \pm \frac{1}{2}$ is shown in Fig. 3. Notice that the holes created by ϵ_2/Z_2 and $\epsilon_3/(Z_2 - \beta_3)$ merge with each other in the middle picture. The same effect can be produced by moving them together at fixed ϵ : when $\beta_3 \rightarrow 0$ these two approach (5). We study this kind of degeneration limit extensively below.

Returning for a moment to our simplest case (3), there are two more distinct degeneration limits given by the two cycles shown:

- As $\epsilon \rightarrow \epsilon_{\text{crit}}$, C_2 becomes small in a throat which is locally $S^2 \times \mathbb{R}$. This is the right geometry to be interpreted as the effect of some strings pinching the brane into a torus. In the case $\alpha = 0$ the brane becomes an equally thin tube all around, approaching the circular spinning string solution

$$Z_1 = \frac{1}{\sqrt{2}} e^{i(t+\sigma)}, \quad Z_2 = \frac{1}{\sqrt{2}} e^{i(t-\sigma)}, \quad Z_3 = 0. \quad (8)$$

The toroidal brane may thus be thought of as an embiggened circular string. But note that all D3-branes described by (1) carry no worldsheet electric field F_{01} , and thus the string solution here is not an F-string.

- As $\epsilon \rightarrow 0$, instead C_1 becomes small in a throat locally $S^1 \times \mathbb{R}^2$. Here it is useful to think of the $\epsilon \neq 0$ function (3) not as

¹ Recall that the notion of a connected sum is this: If cutting a 3-manifold M along an S^2 separates the manifold into $M'_1 \sqcup M'_2$, and M_i is M'_i with a 3-ball glued to its boundary, then we write $M = M_1 \sharp M_2$. The sphere is the identity in the sense $M = M \sharp S^3$. Every (oriented-closed-connected) 3-manifold has a unique decomposition as a sum of prime manifolds, primeness meaning that every separating S^2 bounds a ball.

The connected sum of 2-manifolds, which we write \sharp , is defined by similarly cutting along S^1 . This gives rise to the genus classification of surfaces $S^2, T^2, T^2 \sharp T^2, \sharp^g T^2$.

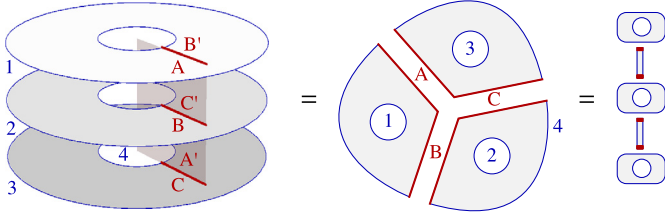


Fig. 4. Branch cut for the (3, 1, 0) case (9). Each sheet of Σ on the left can be turned inside-out to give a wedge as shown. (The numbers label boundary components.) Gluing these back together, the result is a disk with three holes, drawn schematically at the right, and equivalent to Fig. 3(left). (Note that the cuts labelled $A = A'$ etc. are not the S^2 glue lines of the connected sum.)

the addition of a meromorphic term to (2) but (multiplying through by the denominator) as the addition of a small term to a factorised polynomial. That is, $f = Z_1 Z_2 + \epsilon$ describes exactly the same D3-brane as (3), but in the limit $\epsilon \rightarrow 0$ more obviously approaches $f = Z_1 Z_2$, which is a pair of intersecting maximal sphere giants.

The effect of infinitesimal ϵ is localised near to their intersection: At $Z_2 \neq 0$ it changes $Z_1 = 0$ to $Z_1 = \epsilon/Z_2$, perturbing the Z_1 giant smoothly away from maximality (and likewise Z_2). But the effect near to $Z_1 = Z_2 = 0$ is not smooth, as $\sqcup_2 S^3$ is re-connected so as to give topologically $S^2 \times S^1$.

For three poles in (6) (and taking the numbers used in Fig. 3) the view suggested by the limit $\epsilon \rightarrow 0$ is of four intersecting branes, and hence we refer to this as the case (1, 3, 0):

$$\begin{aligned} f(Z_1, Z_2) &= \left(Z_1 - \frac{1}{2}\right) \left(Z_2 + \frac{1}{2}\right) Z_2 \left(Z_2 - \frac{1}{2}\right) \\ &\quad + \epsilon(Z_2^2 - Z_2 - 1) \\ &\approx \left(Z_1 - \frac{1}{2}\right) Z_2 \left(Z_2^2 - \frac{1}{4}\right) + \epsilon'. \end{aligned}$$

The three Z_2 branes intersect the Z_1 brane at different places, and since $\epsilon \neq 0$ modifies the solution appreciably only near to the intersection, it is natural that the effect of several Z_2 branes is very simply related to the effect of one, (14). In the next section we study more general cases in this limit, allowing also several Z_1 branes.

3. Class (m, n, 0)

Fig. 3 above shows Σ for the case (1, 3, 0). Let us now analyse the case (3, 1, 0), which must be equivalent. The simplest example is

$$f = (Z_1^3 - \alpha^3) Z_2 + \epsilon. \quad (9)$$

Solving for $Z_1 = \sqrt[3]{\alpha^3 - \epsilon/Z_2}$, if we again call the area of the Z_2 plane occupied by the solution Σ , this is now a Riemann surface with three sheets. Each sheet is a disk with one hole, and the branch cut (from $Z_2 = 0$ to ϵ/α^3) runs from a point in the hole to a point inside Σ . Drawing the connections as in Fig. 4, it is clear that Σ has three holes, thus we recover $\mathcal{M} = \sharp^3(S^2 \times S^1)$ as desired. The same procedure works equally well for branch cuts of any order.

Before moving on to a new case, we make the following observation: The connected sum of two 3-manifolds \mathcal{M}, \mathcal{N} can be regarded as the effect of connecting a tube $S^2 \times I$ (i.e. S^3 with two punctures) between any point on one and any point on the other:

$$\mathcal{M} \sharp \mathcal{N} = \mathcal{M} \sharp S^3 \sharp \mathcal{N}.$$

Connecting a similar tube between two points on the same manifold \mathcal{M} instead has the effect of adding one term $S^2 \times S^1$:

$$\mathcal{M} + (S^2 \times I \text{ handle}) = \mathcal{M} \sharp (S^2 \times S^1). \quad (10)$$

In the notation of the figures, where $\bigcirc = S^2 \times S^1$ and $\text{---} = S^2 \times I$ tube, this reads

$$\bigcirc \text{---} \bigcirc = \bigcirc \text{---} \bigcirc \text{---} \bigcirc = \sharp^3 \bigcirc.$$

Now consider the case (2, 2, 0), starting with

$$f = (Z_1^2 - \alpha^2)(Z_2^2 - \beta^2) + \epsilon. \quad (11)$$

Clearly Σ has two sheets, each with two holes, connected by a pair of branch cuts. To analyse this, we can split each sheet along surfaces C_i like those used in the previous section – see Fig. 5. This gives two copies of the (2, 1, 0) case, $\sharp^2 \bigcirc$, connected in two places. Re-connecting along C_3 on the upper sheet gives the connected sum of the two pieces, and re-connecting the lower sheet adds a handle of the type just discussed. In all we get

$$\begin{aligned} \mathcal{M} &= [\sharp^2(S^2 \times S^1)] \sharp [\sharp^2(S^2 \times S^1)] + (S^2 \times I \text{ handle}) \\ &= \sharp^5(S^2 \times S^1). \end{aligned}$$

Fig. 5 shows this procedure. Instead of (11) it uses $f = (Z_1^2 - \alpha^2) + \epsilon/(Z_2 - \beta) + i\epsilon/(Z_2 + \beta)$, with $\alpha = \frac{1}{2}$, $\beta = \frac{1}{4}$ and $\epsilon = \frac{1}{9}$, to have a convenient arrangement of branch points. It also shows an alternative argument to check that the choice of how we draw the branch cuts does not matter.

Generalising to the case (m, n, 0), the topology is

$$\mathcal{M} = \sharp^K(S^2 \times S^1), \quad K = mn + (m-1)(n-1). \quad (12)$$

The counting comes from drawing a grid of \bigcirc and connecting horizontally (as in Fig. 3) and vertically (as in Fig. 4).

So far we have assumed that the $m+n$ intersecting branes are all at distinct positions, or in other words we considered only single poles. In the last section, allowing instead higher-order poles (5) did not change the topology, but this is no longer true here. We can investigate this by moving poles to co-incide. There are two ways to do this in (11), taking either $\alpha \rightarrow 0$ or $\beta \rightarrow 0$, and these must be equivalent. Solving for Z_1 , the branch points are located at

$$Z_2 = \pm\beta, \pm\sqrt{\beta^2 + \epsilon/\alpha^2}.$$

For small ϵ the second pair is inside Σ , giving the analysis above. But (holding ϵ fixed and) taking the limit $\alpha \rightarrow 0$, these move off to infinity, giving cuts all the way across Σ . In the limit $\beta \rightarrow 0$, instead the holes in Σ merge into one (as happened in Fig. 3). Both situations are drawn in Fig. 6, and each leads to $\mathcal{M} = \sharp^3(S^2 \times S^1)$.

It is now clear how to treat any set of poles of any order. Write n for the number of separated poles in Z_2 , and N for their total order. (Two double poles thus give $N=4$, $n=2$, as does one single and one triple pole.) Similarly write $M \geq m$ for poles in Z_1 . Drawing an $m \times n$ grid of \bigcirc , the number of vertical connections is M , and horizontal N – see Fig. 7. Then counting the holes we get

$$\mathcal{M} = \sharp^K(S^2 \times S^1), \quad K = 1 + M(n-1) + N(m-1). \quad (16)$$

This change from (12) is a result of holes in Σ merging with each other. We learned in Section 2 that the effect of increasing ϵ is similar. Thus we expect that, for a completely general $\frac{1}{4}$ -BPS giant, the topology will still be $\sharp^K(S^2 \times S^1)$ for some K .

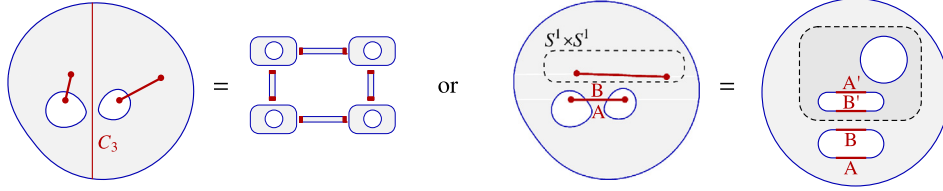


Fig. 5. Branch cuts for case (2, 2, 0). The first plot shows two square-root cuts each of which can be treated as in Fig. 4, giving the vertical connections; the horizontal connections are from the glue line C_3 . The second plot shows the same branch points connected the other way. In this case we can pull the lower sheet of Σ through the cut to obtain the figure on the right. (This happens within the dashed line. The circular boundary component was the outer boundary of the lower sheet.) Now Σ is a disk with three holes plus two handles, giving the same topology.

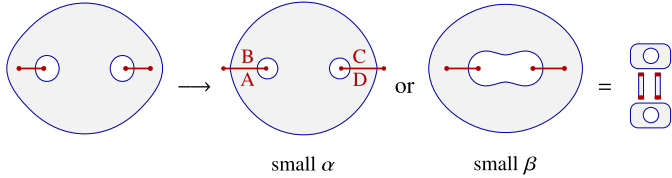


Fig. 6. Degeneration limits of the (2, 2, 0) case (11), drawing always the upper sheet of Σ . For the central picture (small α) we have two disks connected by 4 handles (labelled A...D), while for the right-hand picture (small β) we have 2 tori connected by 2 handles. (The initial picture is $\alpha = \beta = \frac{1}{2}$, $\delta = \frac{1}{10}$, and for each limit drawn 'small' means $\frac{1}{3}$.)

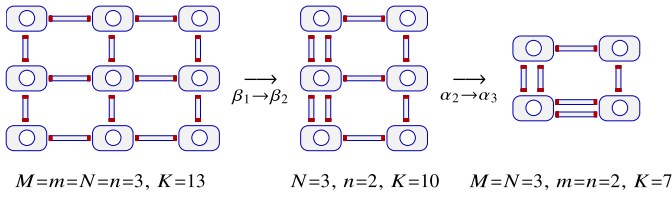


Fig. 7. Degeneration of the case (3, 3, 0). Starting with three distinct poles at $Z_1 = \alpha_i$ and three at $Z_2 = \beta_j$, we first allow two β poles to merge into a double pole, and then two α poles likewise. \mathcal{M} is given by (16) with the numbers shown.

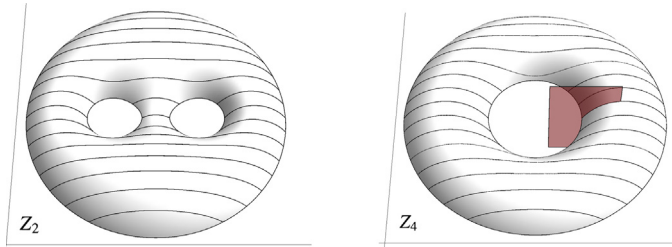


Fig. 8. Plots for the $\frac{1}{8}$ -BPS case (1, 2, 1). The first picture shows Σ drawn as two points fibred over Z_2 . The second shows the upper of two sheets in the $Z_4 = Z_1Z_3$ plane, which are connected by a branch cut drawn in red.

4. Eighth-BPS

We now wish to turn on at least one intersecting Z_3 giant, and take a similar small- ϵ limit. Using what we have learned, we can immediately treat all cases (1, n , 1) together. Consider

$$f = Z_1Z_3 + \epsilon h(Z_2) \quad (13)$$

where h is a function with n poles. Clearly $f = 0$ fixes $\phi_+ = \phi_1 + \phi_3$ and the product r_1r_3 in terms of Z_2 , while $\phi_- = \phi_1 - \phi_3$ is unconstrained. We can solve for r_1 and r_3 as separate functions of Z_2 by writing $\sum_i r_i^2 = 1$ as

$$(r_1 \pm r_3)^2 = 1 - r_2^2 \pm 2r_1r_3 \equiv H_{\pm}$$

and substituting in $r_1r_3 = \epsilon|h|$. This gives

$$(r_1, r_3) = \frac{1}{2}(\sqrt{H_+} \pm \sqrt{H_-}, \sqrt{H_+} \mp \sqrt{H_-}).$$

At a point Z_2 for which $H_- \geq 0$ there are two solutions (coalescing when $H_- = 0$), while for $H_- < 0$ there are none. Notice that where h has a pole, $H_- \rightarrow -\infty$, and thus the neighbourhood of such points will be excluded. (And for small ϵ , each such hole will be small.) Define Σ to be two copies of the area of the Z_2 plane for which $H_- \geq 0$, sewn up along the boundary. For one pole this is a simple torus, while for n poles $\Sigma = \natural^n T^2$.

In the $\frac{1}{4}$ -BPS case we always had an S^1 fibred over Σ , shrinking to a point on $\partial\Sigma$. Fitting with the fact that this boundary is now empty, the ϕ_- circle here never shrinks to a point. To check, note that the metric is

$$ds^2 = \sum_{i=1}^3 (dr_i^2 + r_i^2 d\phi_i^2) = 2(r_1^2 + r_3^2) d\phi_-^2 + \dots$$

Thus for the length of the ϕ_- circle to be zero we need $r_1 = r_3 = 0$, which implies $r_2 = 1$, and this is never part of Σ . We conclude that the topology is

$$\mathcal{M} = (\natural^n T^2) \times S^1. \quad (14)$$

Note that all such three-manifolds are prime – the connected sum here is the two-dimensional one, and to separate the manifold (nontrivially) we must cut along T^2 surfaces.

While the area of the Z_2 plane involved here is not identical to that for the $\frac{1}{4}$ -BPS case of Section 2, the spirit is clearly very similar: each pole increases the genus of the base space Σ . It is natural to ask how much of our analysis of Section 3 still holds. To understand this we begin by re-analysing $f = Z_1(Z_2^2 - \beta^2)Z_3 + \epsilon$, the case (1, 2, 1). Solving for Z_2 we get

$$Z_2 = \pm \frac{\beta \sqrt{Z_1Z_3 - \epsilon/\beta^2}}{\sqrt{Z_1Z_3}}.$$

It is natural to think of this as having a branch cut in the $Z_4 = Z_1Z_3$ plane. Fixing our position on this plane fixes Z_2 up to a choice of sheets, after which we still have (at a generic point) two solutions (r_1, r_3) . Fig. 8 shows the upper-sheet part of Σ which, when glued along the branch cut drawn, gives a double torus, and thus the same topology as before. The angle in the S^1 factor is still $\phi_1 - \phi_3$.

One extension beyond (13) is now fairly obvious. If we consider²

$$f = 1 + \sum_{k=1}^m \frac{\epsilon'_k}{Z_1Z_3 - \gamma_k} + \sum_{j=1}^n \frac{\epsilon_j}{Z_2 - \beta_j}$$

then we can re-use all the $\frac{1}{4}$ -BPS analysis. Just as we replaced Σ of Fig. 3 with two copies glued along their edges to get (14), similarly replace Σ of Figs. 5, 7 with their closed cousins. We get $(\natural^K T^2) \times S^1$ with the same K as before.

² Note aside that we could likewise consider $\frac{1}{4}$ -BPS solutions of the form $f = (Z_1 - \alpha)(Z_4 - \gamma) + \epsilon'$. For small γ this can give a double torus $\natural^2(S^2 \times S^1)$, but small ϵ' here does not guarantee that ϵ in (18) is small.

But it is essential here that f contains only the product $Z_1 Z_3$. The more natural class $(m, n, 1)$ of solutions

$$f = Z_3 + \sum_{i=1}^m \frac{\epsilon'_i}{Z_1 - \alpha_i} + \sum_{j=1}^n \frac{\epsilon_j}{Z_2 - \beta_j}$$

will break the S^1 symmetry in (14). We leave the analysis of this, and completely general $\frac{1}{8}$ -BPS cases, for future work.

5. Conclusion

The main result of this Letter is as follows:

Let $g(Z_1, Z_2)$ be a meromorphic function with m distinct poles at $Z_1 = \alpha_i$, and write M for the number of poles counting multiplicity. Similarly let n and N count the poles at $Z_2 = \beta_j$. We require $m, n \geq 1$, and $|\alpha_i|^2 + |\beta_j|^2 \leq 1 \forall i, j$.³ Consider the $\frac{1}{4}$ -BPS giant described by

$$f(Z_1, Z_2) = 1 + \epsilon g(Z_1, Z_2). \quad (15)$$

For sufficiently small ϵ , this has topology specified by the prime decomposition

$$\mathcal{M} = \sharp^K (S^2 \times S^1), \quad K = 1 + M(n-1) + N(m-1). \quad (16)$$

As ϵ is increased, generically⁴ K will decrease, and the brane may break up into several disjoint pieces. All pieces are either spheres or connected sums of $(S^2 \times S^1)$:

$$\mathcal{M} = \bigsqcup_i^L \sharp^{K_i} (S^2 \times S^1) \bigsqcup_j^{L'} S^3. \quad (17)$$

We found it convenient to deal with a function f with poles, which in some sense repel the base space Σ thus creating holes in the brane.⁵ The same solutions can equivalently be specified by polynomial functions of the form⁶

$$f(Z_1, Z_2) = \prod_{i=1}^m (Z_1 - \alpha_i)^{\mu_i} \prod_{j=1}^n (Z_2 - \beta_j)^{\nu_j} + \epsilon \text{poly}(Z_1, Z_2). \quad (18)$$

Clearly $\epsilon = 0$ gives a factorised f and thus a set of intersecting spherical giants (2). The effect of small ϵ is to suppress all but the simplest kind of interactions: the topology is unchanged when the last term here is replaced by a constant. Nevertheless what we have observed is that the effect of increasing ϵ is quite simple: the tori degenerate (reducing K) and ultimately split into disjoint spheres. Thus we believe that (17) applies to generic polynomial functions $f(Z_1, Z_2)$.

For $\frac{1}{8}$ -BPS geometries we have more limited results. The generalisation which can be treated by borrowing much of the analysis from above is

$$f(Z_1, Z_2, Z_3) = 1 + \epsilon g(Z_4, Z_2), \quad Z_4 = Z_1 Z_3$$

with g defined as in (15). For small enough ϵ the resulting topology is⁷

$$\mathcal{M} = [\sharp^K (S^1 \times S^1)] \times S^1$$

where K is as in (16). Notice that none of these topologies can occur in the $\frac{1}{4}$ -BPS case. Generalising this to allow other combinations of Z_3 branes (such as (18) with $\prod_k (Z_3 - \gamma_k)$ inserted) is an open problem. But it seems clear that the form of \mathcal{M} will change, and in particular will not have an overall S^1 factor.

While our focus in this Letter has been entirely on the classical membranes described by (1), a detailed quantisation of the moduli space of Mikhailov solutions was carried out in [9], and used to draw conclusions about the spectrum of $\frac{1}{8}$ -BPS states in $\mathcal{N} = 4$ SYM. It would be of great interest to pursue the relationship between these results and ours.

This work forms part of a larger research program aimed at understanding how local and global properties of spacetime are encoded in gauge theory. For recent work in this direction, see [10–13] and the references therein. In this context, it would be nice to see how the topologies studied here emerge in operators dual to Mikhailov's giants in SYM. There too, perhaps our small- ϵ limit is likely to be the tractable one.

Acknowledgements

We thank David Berenstein, Robert de Mello Koch, Jan Gutowski, Konstadinos Sfetsos, Jonathan Shock and Alessandro Torielli for discussions.

M.C.A. is supported by a UCT URC postdoctoral fellowship. J.M. acknowledges support from the NRF of South Africa under the HCDE and IPRR programs. N.R. is supported by a DAAD-AIMS scholarship, and a DAAD short-term research fellowship.

References

- [1] J.M. Maldacena, The large N limit of superconformal field theories and supergravity, *Adv. Theor. Math. Phys.* 2 (1998) 231–252, arXiv:hep-th/9711200.
- [2] N. Beisert, et al., Review of AdS/CFT integrability: An overview, *Lett. Math. Phys.* 99 (2012) 3–32, <http://dx.doi.org/10.1007/s11005-011-0529-2>, arXiv:1012.3982.
- [3] J. McGreevy, L. Susskind, N. Toumbas, Invasion of the giant gravitons from anti-de Sitter space, *J. High Energy Phys.* 0006 (2000) 008, arXiv:hep-th/0003075.
- [4] V. Balasubramanian, M. Berkooz, A. Naqvi, M.J. Strassler, Giant gravitons in conformal field theory, *J. High Energy Phys.* 0204 (2002) 034, <http://dx.doi.org/10.1088/1126-6708/2002/04/034>, arXiv:hep-th/0107119.
- [5] S. Corley, A. Jevicki, S. Ramgoolam, Exact correlators of giant gravitons from dual $\mathcal{N} = 4$ SYM theory, *Adv. Theor. Math. Phys.* 5 (2002) 809–839, arXiv:hep-th/0111222.
- [6] R. de Mello Koch, J. Murugan, Emergent spacetime, in: *Foundations of Space and Time Workshop*, Cape Town, August 2009, 2009, pp. 164–184, arXiv:0911.4817.
- [7] A. Mikhailov, Giant gravitons from holomorphic surfaces, *J. High Energy Phys.* 0011 (2000) 027, <http://dx.doi.org/10.1088/1126-6708/2000/11/027>, arXiv:hep-th/0010206.

⁷ From the topologies written down here it is trivial to obtain the homology groups. The Betti numbers are:

$$\frac{1}{4}\text{-BPS: } b_0 = b_3 = 1, \quad b_1 = b_2 = K,$$

$$\frac{1}{8}\text{-BPS: } b_0 = b_3 = 1, \quad b_1 = b_2 = 2K + 1.$$

For the case (1, 1, 0), the generators of H_1 and H_2 are cycles C_1 and C_2 in Fig. 1. It is easy to draw similar cycles in Fig. 3's case (1, 3, 0). Similar cycles drawn in Fig. 8's case (1, 2, 1) will all be 1-cycles.

³ We could weaken this condition to allow for cases where not every pair of branes intersects in the limit $\epsilon \rightarrow 0$; this has the effect of deleting some nodes from the corners of the lattice shown in Fig. 7, and thus reducing K , but not otherwise changing the topology.

⁴ This is true if the residues of g are constants, in which case $\sum_i K_i \leq K$ and $L + L' \leq MN$ in (17). But if the numerator of g is of sufficiently high order then K may increase.

⁵ The poles are thus never on the worldvolume, so f is locally analytic, which is enough to guarantee a solution to the equations of motion from (1).

⁶ Here $M = \sum_i \mu_i$ and $N = \sum_j \nu_j$.

- [8] A. Mikhailov, Nonspherical giant gravitons and matrix theory, arXiv:hep-th/0208077.
- [9] I. Biswas, D. Gaiotto, S. Lahiri, S. Minwalla, Supersymmetric states of $\mathcal{N} = 4$ Yang–Mills from giant gravitons, J. High Energy Phys. 0712 (2007) 006, <http://dx.doi.org/10.1088/1126-6708/2007/12/006>, arXiv:hep-th/0606087.
- [10] J. Pasukonis, S. Ramgoolam, From counting to construction of BPS states in $\mathcal{N} = 4$ SYM, J. High Energy Phys. 1102 (2011) 078, [http://dx.doi.org/10.1007/JHEP02\(2011\)078](http://dx.doi.org/10.1007/JHEP02(2011)078), arXiv:1010.1683.
- [11] R. de Mello Koch, S. Ramgoolam, A double coset ansatz for integrability in AdS/CFT, J. High Energy Phys. 1206 (2012) 083, [http://dx.doi.org/10.1007/JHEP06\(2012\)083](http://dx.doi.org/10.1007/JHEP06(2012)083), arXiv:1204.2153.
- [12] J. Pasukonis, S. Ramgoolam, Quantum states to brane geometries via fuzzy moduli spaces of giant gravitons, J. High Energy Phys. 1204 (2012) 077, [http://dx.doi.org/10.1007/JHEP04\(2012\)077](http://dx.doi.org/10.1007/JHEP04(2012)077), arXiv:1201.5588.
- [13] D. Berenstein, Giant gravitons: a collective coordinate approach, Phys. Rev. D 87 (2013) 126009, <http://dx.doi.org/10.1103/PhysRevD.87.126009>, arXiv:1301.3519.